Behavior of Damaged Continuous Reinforced Concrete Beams Repaired by CFRP Sheets

Alaa Y. Alkinani[1, a*] and Hayder H. Kamonna[1, b]

[1]Department of Civil Engineering, University of Kufa, Kufa, Iraq

[a] alaay.alkinani@student.uokufa.edu.iq and [b] hayder.kammona@uokufa.edu.iq

*Corresponding author

Abstract. Despite the widespread use of RC continuous beams, the performance of these beams, when repaired via Fiber Reinforced Polymer (FRP) composite material, has received less attention. Furthermore, several features of the flexural aspect of repaired RC continuous beams still demand experimental and analytical evaluation. However, many anchoring methods have been developed to delay premature failure in the RC beams, which are strengthened with FRP composite materials. The plan of this experimental study consists of eight continuous beams cast with dimensions (150*250*2800) mm considering the length of the clear span is 1300mm. Except for one, all specimens were attached via Carbon FRP sheets about 70% of the span length in negative and positive moment zones beyond a predetermined damage level. Moreover, this study suggested modifying the end-anchor technique and adding CFRP layers with (45, 65, and 95) % as damage ratios. According to the results, the optimal percentage of restored ultimate capacity was 108.8% with peeling-off concrete cover failure mode, which was obtained from using an end-anchor and two layers of the sheet. Also, increasing the damage ratio leads to a decline in toughness and ductility values. In addition, it is possible to repair the structure with a 95% damage ratio rather than remove it.

Keywords: CFRP; damage ratios; end-anchor; RC continuous beam; repaired beam.

1. INTRODUCTION

One of the effective approaches for strengthening and repairing RC structures is the external application of fiber-reinforced polymer (FRP) composite materials using epoxy on the surface of reinforced concrete elements[1,2]. There has been a considerable increase in the effective applications of FRP strips in the flexural reinforcement of concrete structures over the past two decades, which has benefited their efficiency [3]. Recently, the importance of repairing RC structures has increased dramatically, which may be attributed to the world's endeavor to eliminate concrete rubbish from the environment (sustainability). Common forms of degradation that cause damage to many reinforced concrete structures include cracks and deflections, which are affected by a wide range of factors, such as earthquakes, corrosion of reinforced bars, changes in the natural environment, and vibrations [4]. Although ductility is more important, especially in indeterminate structures like continuous beams, it permits moment redistribution through plastic hinge rotations. Several studies found that FRP-strengthened continuous beams increased loading capacity but decreased ductility [5,6].

Because of the rising need for upgrading concrete buildings, the external bonding of FRP composites has become an emerging structural strengthening approach due to their high tensile strength, low weight, simple installation, and corrosion resistance[7]. Hamrat et al. [8] demonstrated experimentally that adding more than one layer of FRP laminates/sheets reduced the mid-span deflection of repaired beams by (15–35) % and enhanced ultimate load capacity by (13–100) %. Whereas preloading 100% and 90% of beams attached by CFRP materials improves load capacity by 51.5% and 68.5%, as observed by Hamed et al. [9]. As the ratio of CFRP's width to concrete's width rose, the stiffness and ultimate load for the inverted T-beams reinforced with CFRP increased. Also, the ultimate load capacities of beams attached by CFRP improved by 4-90 percent when increasing the number of layers, but the ductility was reduced [10]. Bengar and Maghsoudi [5] concluded that in beams that are strengthened by CFRP, increasing the number of layers decreases the ultimate strain and increases the ultimate capacity of load. Moreover, they found that the moment redistribution and load capacity increased considerably via using the end anchor technique. Mohammed and Kadhim [11] observed that Increasing the number of CFRP layers reduced the loss in stiffness of strengthened beams after yielding the tensile steel, and the defection ductility index was decreased. In addition, when using more layers of CFRP sheets for strengthening reinforced concrete beam, the ultimate capacity can grow to 170.2% of the strength of the control beam, summarized by reference [12].

The objective of the present study was to provide an improved strategy to assess the flexural strengthening of reinforced concrete continuous beams repaired via attaching by CFRP sheet. In addition, to investigate the impact of using the end anchors in positive and negative zones, adding more layers, and different damage levels in the continuous beams through discussing ductility, crack pattern, load versus deflection curve, and toughness.

2. EXPERIMENTAL WORK

The ready concrete mixture for eight RC continuous beams was made of five resistant Portland cement materials: fine aggregate (passing from 4.75 mm and remaining on 0.075 mm), coarse aggregate with 19 mm maximum size, superplasticizer, and water. For 28 days, the average compression strength test of three cubes

(150*150*150) mm recorded 44 MPa, the tensile strength test of three cylinders (100*200) mm achieved 3.8MPa, and flexural strength for three prisms (100*100*400) mm showed 6.1MPa. The cross-section for the continuous beams was (150*250) mm and length (2800) mm with 1300 mm for a clear span, and the clear concrete cover was chosen to be 30 mm. Furthermore, all specimens with the same size and compressive strength were constructed by additional transverse reinforcement to ensure the possibility of bending failure. Two bars of 10 mm in diameter for both tension and compression parts in longitudinal steel reinforcement, but in transverse steel reinforcement, the bar diameter was 10 mm with 100 mm for the spacing. In addition, the tensile and yield strength were 670 and 603 MPa, respectively. Regarding the mechanical characteristics of CFRP sheets, the tensile strength of Sika Wrap 300-C was 4000 MPa with 0.167 mm thickness. While for epoxy Sikadur 330 [13], the tensile strength was 30 MPa with 1.3 kg/L density. The first beam (B1), not bonded by CFRP sheets and tested to failure, was selected as the control. Three specimens (B2, B5, B6) were loaded with 45% ultimate load of the control, the other three (B7, B10, B11) were damaged by 65%, and the last one (B12) was preloaded with 95%. After the preloading stage, some processes were followed to attach the CFRP sheet to the surface of the specimens, which are illustrated clearly in Figure 1.

(a) (b) (c)

Figure 1: Different steps for preparing the specimen: (a) the beam surface was grinding by flap disk (b) the specimen was washed by water (c) 50 mm as constant width of CFRP sheets and epoxy were glued on the beam surface.

The procedure of designing a continuous beam according to ACI318-19 was based on calculating ρ_{min} and then the ultimate moment; after that, from the bending diagram, the maximum moment was chosen to equal the ultimate value to find P. This P was multiplied by 2.5 to ensure the occurrence of flexural failure; then, this value will be chosen as a V_u to design the shear. Finally, the reinforcement limit and detailing were checked by finding $S_{max\ as}$ illustrated in Figure 2 (a). The style of the bonding CFRP sheets was chosen as a 0.7L in tension part on both positive and negative moment zones regarding covering the maximum moment in the bending moment diagram, as shown in Figure 2 (c).

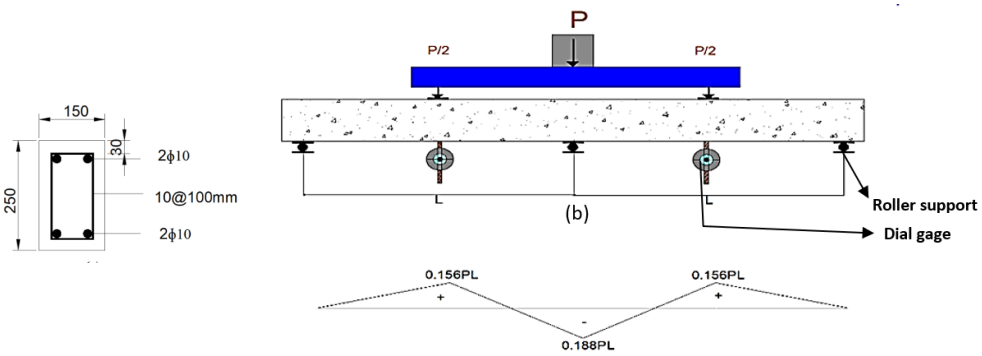

(a) (c)

Figure 2: The cross-section and the loading applied on the continuous beam with bending moment diagram.

Whereas the L_{span}/L_{sheet} in B2 and B7 was 0.7 in both the sagging and hogging moment regions glued by epoxy, as illustrated in Figure 2 (a). The same last bonding style bonded B5, B10, and B12 by adding anchors at the ends of CFRP sheets, as shown in Figure 2 (b). In contrast, the difference point between Figure 3 (b) and (c) was adding one more layer of the sheet which has been done in B6 and B11. In terms of cost, when using more than layers, the increment was 19%.

For a specimen with one layer, the cost of (CFRP+ epoxy+ bonding wage) = 48$

For a specimen with two layers, the cost of (CFRP+ epoxy+ bonding wage) = 57$

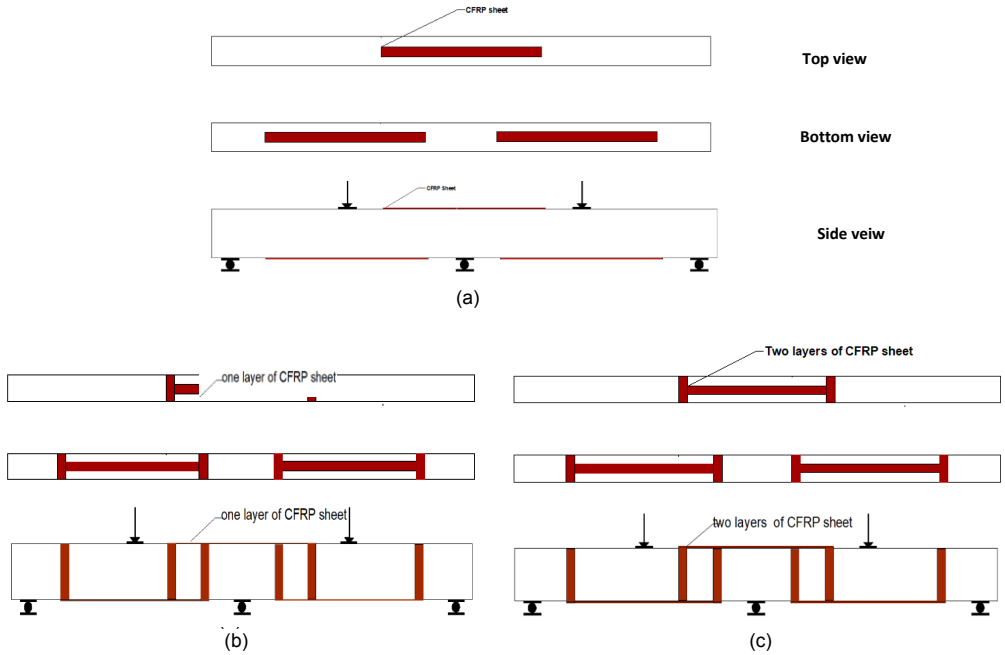

Figure 3: The ways of repair method for seven continuous beams.

As for the testing continuous beam, it is shown in Figure 4. The type of support was a roller, and the loading was contributed through two metal plates.

Figure 4: Control under the compression hydraulic machine.

3. CRACK PATTERN

In this part, the map of the propagation of the cracks will be explained through Table 1 and the following Plates from (3 to10) of beams particularly.

Table 1: The ultimate capacity for specimens with the restored ratio.

Beams	Names	Load, kN	% Ratio of restored capacity	Deflection, mm
B1	control	285	------	10.9
B2	N45-p0.7L-n0.7L-1L	290	101.7	8.91
B5	A45-p0.7L-n0.7L-1L	240	84.2	9.43
B6	A45-p0.7L-n0.7L-2L	310	108.8	10.5
B7	N65-p0.7L-n0.7L-1L	280	98.2	7.81
B10	A65-p0.7L-n0.7L-1L	240	84.2	8.9
B11	A65-p0.7L-n0.7L-2L	280	98.2	7.2
B12	A95-p0.7L-n0.7L-1L	270	94.7	7.43

N, A: Non-anchor and anchor.
45, 65, 95: Damage ratio%.
p, n: Positive and negative moment regions.
L: Length of one span center to center.
1L, 2L: layers of CFRP sheets.

3.1 CONTROL Specimen (B1)

The first specimen was without strengthening, which was considered the control specimen. The result explained that the failure was flexural in a conventional manner. However, the first visible crack in a specimen (B1) occurred at a load of around 30% of its ultimate load at the top of the middle support because this region had the greatest moment. When the load was raised, flexural cracks expanded in depth, width, and number. At the stage of cracking, the cracks grew in two-sided positive and one-side negative moment zones in the continuous beam regularly. The flexural cracks propagated toward the compression part slightly. It was clear to notice that there were small inclined shear cracks that emerged accompanying the flexure cracks. Furthermore, concrete crashing happened under plate loading in the center of spans in 285 kN, as shown in Figure 5. This refers to the tension (steel bars) yielded, and then the compression (concrete) failed.

Figure 5: Map of cracks for control.

3.2 Specimen B2 (N45-p0.7L-n0.7L-1L)

The external bonding of the CFRP sheet in this beam was equal to 0.7L for both negative and positive zones with one layer with a preloading ratio of 45%. At the second tested stage, it can be observed that when the applied load increased, there were a series of small shear cracks through the side view of the beam. Compared with the reference beam, 101.7% of the capacity was restored when the mentioned repairing configuration was adopted. Also, it was capable of withstanding load failure 290 kN. From the map of crack propagation in Figure 6, it can be observed the first crack appeared at 13.8% of the ultimate load in the region of maximum moments. Furthermore, some cracks began to become clear with an angle of more than 45^{o}, but then they tended to take the straight path. This may be classified as shear-flexural cracks.

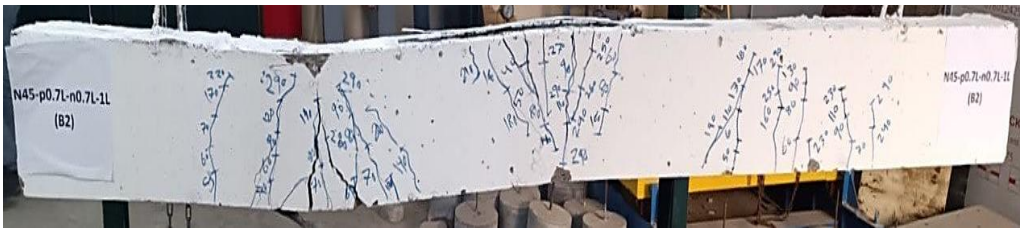

Figure 6: Map of cracks for N45-p0.7L-n0.7L-1L

3.3 Specimen B5 (A45-p0.7L-n0.7L-1L)

This beam was initially loaded to about 45%Po, and then the specimen was repaired as the N45-p0.7L-n0.7L-1L specimen but adopted end anchors at each end of each sheet. From Figure 7, It behaved as like the control beam during the first loading phase. At a load of about 20 kN, the first crack appeared obviously in the middle beam and mid-right span at the tension face. Furthermore, many cracks tend to initiate straightly. In the

left mid-span, there was a widened crack that appeared at 50 kN, and it kept penetrating the concrete block vertically until 240 kN, resulting in specimen failure.

Figure 7: Map of cracks for A45-p0.7L-n0.7L-1L.

3.4 Specimen B6 (A45-p0.7L-n0.7L-2L)

This beam has been initially loaded up to 45%ultimate load. During the first stage of loading, the specimen showed a similarity in behavior with the control beam. As in Figure 8, the first crack appeared straightly with 90^{o} at 7.4% from the ultimate load in the center of the two spans at the tension face. It is clear that the vertical cracking shifted considerably to be diagonal at 29% of its ultimate load and penetrated through all the depth of the concrete section. The cracks tended to expand and enlengthen towards the compression zone in the maximum moment area. Furthermore, a crack formed near the plate loading and expanded horizontally with the cover of concrete and after that, it stretched upwards with the peeling of the cover, causing the failure of the beam. Compared with the control specimen, it can be noted that the restored capacity was about 108.8%, which is the largest value. This may be attributed to the small value of the initial loading and the use of two layers of CFRP with anchors.

Figure 8: Map of cracks for A45-p0.7L-n0.7L-2L.

3.5 Specimen B7 (N65-p0.7L-n0.7L-1L)

This specimen was loaded initially with a load level of 65% of the failure load of the control specimen before the repairing process. After reaching the predetermined level of loading, the load is removed, and the specimen is retrofitted on each side. Then, it is subjected to the second stage of loading. Figure 9 shows the crack pattern. It is observed as the load increases. The first crack appeared at 7.1% from the failure load. A clear flexural crack and a few shear cracks diagonally oriented directly to the compression zone. At 90% of the final loading stage, a sudden sheet rupture occurred at the positive moment section. Where the cracks were able to expand and achieve a flexural path failure. The specimen (N65-p0.7L-n0.7L-1L) could withstand load up to 280 kN with rupturing in the CFRP sheet.

Figure 9: Map of cracks for N65-p0.7L-n0.7L-1L.

3.6 Specimen B10 (A65-p0.7L-n0.7L-1L)

185 kN was the load applied to this specimen before using 0.7L of the CFRP sheets with an end-anchor. After the repairing stage, 30 kN was the first cracking load in both mid-pans. However, more cracks were clear in the left span with an angle of more than 80^{o}, all of them extending towards the loading source. When the load increased, the sheet debonding happened, and the crushing concrete appeared, which led to failing the specimen with high noise was heard. The map of the crack pattern is explained clearly in Figure 10.

Figure 10: Map of cracks for A65-p0.7L-n0.7L-1L.

3.7 Specimen B11 (A65-p0.7L-n0.7L-2L)

This model of bonding used the U shape of an anchor wrapped in two layers of CFRP after preloading 65% of the ultimate control load. Firstly, two cracks were initiated in the center of both spans at loading 30 kN vertically. Then, a flexure crack appeared from the top of the beam center at 60 kN. As it is obvious, the shear-flexural cracks started to appear close to flexure cracks with inclined at different angles at increasing the load. In addition, it continued to extend significantly until three-quarters of the beam height and then stopped. All cracks were directed toward the sources of the applied loads. At the same time, the cracks continued to expand until the sudden peeling failure of the concrete cover occurred at a loading of 280 kN. Figure 11 shows the crack propagation history of this beam.

Figure 11: Map of cracks for A65-p0.7L-n0.7L-2L.

3.8 Specimen B12 (A95-p0.7L-n0.7L-1L)

95% was the percentage of damage for this specimen, and then it was externally bonding one layer of the CFRP sheet with an anchor at the ends. At 30 kN, the crack began to appear in the center of the continuous beam spans. However, a clear vertical crack can be noted in the middle of the negative moment area with an inclined crack accompanying it. Some cracks propagated by an angle of more than 60 were directed to the compression part. The concrete cover started to peel, causing the failure for the specimen with the restored force of about 94.7% of the control model, as well as. There was no crushing of concrete at the loading and supporting points, as illustrated in Figure 12.

Figure 12: Map of cracks for A95-p0.7L-n0.7L-1L.

4. LOAD-DEFLECTION CURVE

From Figure 13, it can be observed that the load changes in the first zone of the CONTROL beam from (0 to 30) % of its ultimate capacity, which is called the linear-elastic zone and is characterized by no cracking anymore and the greatest stiffness. However, the second zone shows that the load values range from (30 to 77) % of its ultimate capacity, and the cracks start to appear in the tension faces of the concrete block and steel bar, still within the elastic limit. In other words, the steel bar bears the majority of the loading. This stage is typically what is called service behavior. It is characterized by small degradation in the beam stiffness. In the third zone, the load value changes from 77% of its ultimate capacity to the loading level at which the beam fails, an ultimate stage, which means the concrete crushes in compression face for the location right and left depending on where the concrete is crushing in terms of strains. In this zone, a flat load-deflection curve could be obtained. With regard to the deflection of specimens, which loaded (45, 65, and 95) % were (3.23, 4.6, and 9.1) mm, it was the same value for the other beams.

Nevertheless, all these previous stages happened for the repaired beams except the first zone because the specimens entered the cracking stage before the repair. In other words, all tested beams revealed similar

behavior in the uncracked elastic region, indicating that their stiffness values prior to cracking were very similar. Firstly, Figure 13 (a) shows the load versus deflection for the three beams with a 45% damage level. For B2, B5, and B6. It can be observed that the slope of the curve (stiffness) starts to drop at 80% progressively because additional cracks appeared in the concrete block. In addition, the important thing to note from Figure 13 (a) is that B6 failed at 310 kN, the largest load capacity. Secondly, For B7, B10, and B11, the behavior of the three beams looks like the control beam until 100 kN. Then, the stiffness tends to reduce at 220, 170, and 210 kN, respectively, as demonstrated in Figure 13 (b). After this stage, the major point was to achieve high ultimate with a small deflection in B11, which may be related to its effective type of strengthened way. Finally, the stiffness of B12 was less than others at the beginning until 130 kN, and after that, the slope started to grow swiftly till failure. While there was, some softening occurred at the early and final stages for both B5 and B10.

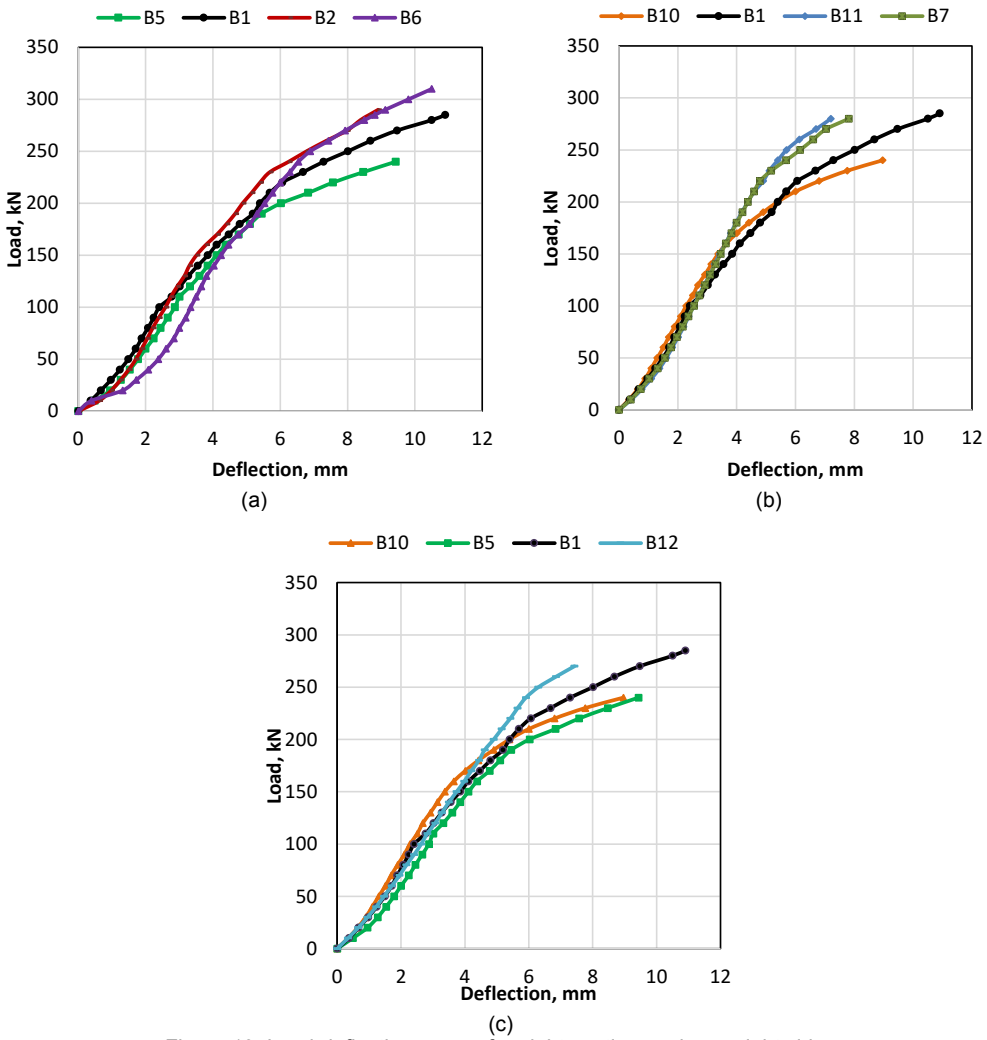

Figure 13: Load-deflection curves for eight continuous beam right sides

5. TOUGHNESS

Flexural toughness is a measure of the capacity to absorb energy; alternatively, it is the capability to resist crack opening performance, that is, the region under the load-deflection curve when stiffness is higher than or equal to zero. The values of toughness calculation for the testing of continuous beams are shown in Table 2, and it is estimated by using the trapezoidal integration method, which is an approximated method. The control beam recorded a toughness of 1927 kN.mm, which is the highest possible value, because of the presence of the Carbon-FRP sheets, which show a brittle response and produce less warning before failure, as well as the surface beam-fixed method for sheets. Generally, the specimens with a damage ratio of 45% produce a lower reduction in toughness than those with other ratios due to the number of cracks being smaller in this stage. Finally, the toughness value of B12 achieved 1076 kN.mm, which was the highest loss value in toughness.

Furthermore, the reason for that may be related to the high damage ratio (95%), which tends to eliminate the beam's efficiency to dissipate the energy. In brief, when the damage ratio increases, the toughness value starts to decrease.

Table 2: The toughness value for testing specimens.

Beam	Names	Area, mm²	% Reducing	Failure modes
B1	CONTROL	1927	-----	Flexural failure
B2	N45-p0.7L-n0.7L-1L	1463	24	Debonding failure
B5	A45-p0.7L-n0.7L-1L	1380	28	Debonding failure
B6	A45-p0.7L-n0.7L-2L	1786	7	Peeling cover
B7	N65-p0.7L-n0.7L-1L	1232	36	Tensile rupture
B10	A65-p0.7L-n0.7L-1L	1370	29	Debonding failure
B11	A65-p0.7L-n0.7L-2L	1080	43	Peeling cover
B12	A95-p0.7L-n0.7L-1L	1076	44	Peeling cover

6. DUCTILITY

The capacity of a structure to endure inelastic deformation without considerably decreasing its strength until failure is described as ductility. In the present study, Δy has been assumed as the displacement from an equivalent elastic-plastic system with reduced stiffness by the secant about 75% of the ultimate lateral load (Pu) of the real system. Moreover, the ductility index ($\Delta\boldsymbol{\mu}$) is predicted according to Park [14] as in Table 3. It is notable that the ductility is reduced obviously when increasing the damage ratio. With regard to the high losing ductility index in B6 and B11, which can be shown by increasing the number of layers, this may be attributed to the CFRP sheets being a brittle material, subsequently leading to minimizing the inelastic capacity of the continuous beam.

Table 3: The ductility index for testing specimens.

Beam	Specimens	Δy (mm)	Δu (mm)	Ductility index $\boldsymbol{\mu}$	$\Delta\boldsymbol{\mu}$ (%)
B1	Control	7.75	10.9	1.406	--------
B2	N45-p0.7L-n0.7L-1L	7.05	8.91	1.263	-10.1
B5	A45-p0.7L-n0.7L-1L	6.72	9.43	1.403	-0.2
B6	A45-p0.7L-n0.7L-2L	8.38	10.5	1.252	-10.8
B7	N65-p0.7L-n0.7L-1L	6.2	7.81	1.259	-10.4
B10	A65-p0.7L-n0.7L-1L	6.35	8.9	1.401	-0.3
B11	A65-p0.7L-n0.7L-2L	6.05	7.2	1.19	-15
B12	A95-p0.7L-n0.7L-1L	6.62	7.43	1.122	-20.1

7. CONCLUSIONS

Based on the summary of tests conducted on the eight reinforced concrete continuous beams repaired with CFRP, we may make the following findings:

- When the damage ratio decreased, an accepted lower limit of ductility index was observed for all continuous beams repaired by CFRP sheets.
- By using two layers of sheets and an end anchor, the restored ratio of the load enhanced, especially in damage level 45%, recorded at 108.8%, as well as the failure mode peeling off the concrete cover.
- The repair continuous beam's toughness value is reduced by increasing the damage percentage.
- For a 95% damage ratio, the repairing process restored about 94.7% of the beam capacity, which may indicate the possibility of repairing the structure rather than removing it.

REFERENCES

[1] J. G. Teng, J. F. Chen, S. T. Smith, and L. Lam. FRP : Strengthened RC Structures. 2023. [Online]. Available: https://ui.adsabs.harvard.edu/abs/2002frp.
[2] H. A. Bengar and A. A. Shahmansouri. A new anchorage system for CFRP strips in externally strengthened RC continuous beams. J. Build. Eng. 2020; 30(1): 101230.
[3] E. Coakley, J. Cairns, K. S. Lee, J. Cairns, and E. Coakley. Ultimate strength of continuous beams with exposed reinforcement. 2013; 11(1): 238–250. doi: 10.3151/jact.11.238.
[4] M. M. Fayyadh and H. A. Razak. Assessment of effectiveness of CFRP repaired RC beams under different damage levels based on flexural stiffness. Constr. Build. Mater. 2012; 37(1): 125–134.
[5] H. A. B. Æ. A. A. Maghsoudi. Experimental investigations and verification of debonding strain of RHSC continuous beams strengthened in flexure with externally bonded FRPs. 2010. doi: 10.1617/s11527-009-9550-7.
[6] A. F. Ashour, S. A. El-Refaie, and S. W. Garrity. Flexural strengthening of RC continuous beams using CFRP laminates. Cem. Concr. Compos. 2004; 26(7): 765–775. doi: 10.1016/j.cemconcomp.2003.07.002.
[7] O. Benjeddou, M. Ben Ouezdou, and A. Bedday. Damaged RC beams repaired by bonding of CFRP laminates. Construction and building materials. 2007; 21(1): 1301–1310.
[8] M. Hamrat et al. Experimental and numerical investigation on the deflection behavior of pre-cracked and repaired reinforced concrete beams with fiber-reinforced polymer," Constr. Build. Mater.2020; 249(1):

118745.
[9] A. Adel, A. Hamed, and K. F. O. El-kashif. Flexural strengthening of preloaded reinforced concrete continuous beams : An experimental investigation. Alexandria Eng. J. 2019; 58(1): 207–216.
[10] A. Al-Khafaji and H. Salim. Flexural strengthening of RC continuous t-beams using CFRP. Fibers. 2020; 8(6): 1–18.
[11] M. Mohammed and A. Kadhim. Behavior of HSC Continuous Beam. . Journal of THERMOPLASTIC COMPOSITE MATERIALS. 2012; 25(1): 33–44.
[12] H. Toutanji, L. Zhao, and Y. Zhang. Flexural behavior of reinforced concrete beams externally strengthened with CFRP sheets bonded with an inorganic matrix. Engineering structures. 2007; 28(1): 557–566.
[13] https://usa.sika.com/content/dam/dms/us01/0/sikadur_-330.pdf
[14] R. Park. Ductility evaluation from laboratory and analytical testing. Proceedings of the 9th World Conference on Earthquake Engineering. 1988. [Online]. Available: http://www.iitk.ac.in/nicee/wcee/article/9_vol8_605.pdf